J. Am. Chem. Soc. **2000,** *122,* 8187−8191

Electron Tunneling through Water: Oxidative Quenching of Electronically Excited $Ru(tpy)_2^{2+}$ (tpy = 2,2′:6,2″-terpyridine) by Ferric Ions in Aqueous Glasses at 77 K

Adrian Ponce, Harry B. Gray,* and Jay R. Winkler*

Contribution from the Beckman Institute, California Institute of Technology, Pasadena, California 91125

Received January 3, 2000

Abstract: The luminescence lifetime of $Ru(tpy)_2^{2+}$ (tpy = 2,2′:6,2″-terpyridine) is 8.0 μs in H_2SO_4/H_2O and HSO_3F/H_2O glasses (25% v/v) at 77 K, and 10.2 μs in D_2SO_4/D_2O (25% v/v). Addition of moderate concentrations of the powerfully oxidizing $Fe(OH_2)_6^{3+}$ ion to the glasses leads to accelerated and highly nonexponential $^*Ru(tpy)_2^{2+}$ decay kinetics. The quenching is attributed to electron transfer from $^*Ru(tpy)_2^{2+}$ to randomly dispersed $Fe(OH_2)_6^{3+}$ complexes. The luminescence decay kinetics and quantum yields in the three aqueous glasses indicate that the electron-transfer rate constants decrease from $\sim10^{13}$ s^{-1} at van der Waals contact with an exponential distance decay constant of 1.68 ± 0.07 Å^{-1}.

Introduction

Electron transfers (ETs) are the only chemical reactions that proceed at significant rates when the reactants are separated by long distances (>10 Å).[1−4] The wealth of experimental data accumulated during the past three decades provides a remarkably uniform picture of long-range ET; rates (k_{ET}) decrease exponentially with increasing donor−acceptor separation (R).[5−12] Superexchange-coupling models provide a theoretical rationale for this behavior,[13−16] defining an exponential distance decay constant (β) that is sensitive to the composition of the medium separating the electron donor (D) and acceptor (A). Large values of β (3−5 Å^{-1}) are expected when D and A are separated by a vacuum because the direct electronic interaction between redox sites decays rapidly with increasing R.[17,18] Superexchange coupling via hole and/or electron states of an intervening medium will facilitate long-range transfers; indeed, β values in the range 0.8−1.2 Å^{-1} have been obtained from experimental investigations of intramolecular ET in donor−bridge−acceptor (D−br−A) complexes.[5−10] Analyses of the D−br−A data tend to focus on superexchange coupling via states of the covalent bridges alone. Experiments on D−br−A complexes with C-shaped bridges, however, indicate that electronic coupling through solvent molecules can be an important factor.[19−22]

Owing in part to a lack of data, the roles of solvent hole and electron states in mediating long-range couplings in D−br−A complexes are not well understood.[23−25] Unique challenges confront the measurement of the ET coupling properties of solvents. In fluid solution, when the positions of D and A are not constrained by a covalent bridge, diffusion places an upper limit on the time scale ($<10^{-9}$ s) and, therefore, the distance range (<9 Å for $\beta = 1.0$ Å^{-1}) for electron tunneling. Nevertheless, analyses of nonexponential fluorescence-quenching kinetics are consistent with $\beta = 1.2 \pm 0.2$ Å^{-1} for tunneling through fluid organic solvents.[26] Longer tunneling distances can be examined if D and A are immobilized. Pulse radiolysis and photochemical investigations of intermolecular electron transfer in aqueous and organic glasses have produced β values in the 0.75−1.4 Å^{-1} range.[4,27,28]

Although immobilizing D and A eliminates the problem of diffusion, it introduces complications into the analysis of the

---

(1) Winkler, J. R.; Nocera, D. G.; Yocom, K. M.; Bordignon, E.; Gray, H. B. *J. Am. Chem. Soc.* **1982**, *104*, 5798−5800.

(2) Calcaterra, L. T.; Closs, G. L.; Miller, J. R. *J. Am. Chem. Soc.* **1983**, *105*, 670−671.

(3) McGourty, J. L.; Blough, N. V.; Hoffman, B. M. *J. Am. Chem. Soc.* **1983**, *105*, 4470−4472.

(4) Miller, J. R.; Beitz, J. V.; Huddleston, R. K. *J. Am. Chem. Soc.* **1984**, *106*, 5057−5068.

(5) Wasielewski, M. R. In *Distance Dependencies of Electron-Transfer Reactions*; Fox, M. A., Chanon, M., Eds.; Elsevier: Amsterdam, 1988.

(6) Closs, G. L.; Calcaterra, L. T.; Green, N. J.; Penfield, K. W.; Miller, J. R. *J. Phys. Chem.* **1986**, *90*, 3673−3683.

(7) Warman, J. M.; Smit, K. J.; de Haas, M. P.; Jonker, S. A.; Paddon-Row, M. N.; Oliver, A. M.; Kroon, J.; Oevering, H.; Verhoeven, J. W. *J. Phys. Chem.* **1991**, *95*, 1979−1987.

(8) Langen, R.; Chang, I.-J.; Germanas, J. P.; Richards, J. H.; Winkler, J. R.; Gray, H. B. *Science* **1995**, 268, 1733−1735.

(9) Smalley, J. F.; Feldberg, S. W.; Chidsey, C. E. D.; Linford, M. R.; Newton, M. D.; Liu, Y.-P. *J. Phys. Chem.* **1995**, *99*, 13141−13149.

(10) Gray, H. B.; Winkler, J. R. *Annu. Rev. Biochem.* **1996**, *65*, 537−561.

(11) Moser, C. C.; Page, C. C.; Chen, X.; Dutton, P. L. *JBIC* **1997**, 2, 393−398.

(12) Williams, R. J. P. *JBIC* **1997**, 2, 373−377.

(13) McConnell, H. M. *J. Chem. Phys.* **1961**, *35*, 508−515.

(14) Curtiss, L. A.; Naleway, C. A.; Miller, J. R. *Chem. Phys.* **1993**, *176*, 387−405.

(15) Liang, C.; Newton, M. D. *J. Phys. Chem.* **1992**, *96*, 2855−2866.

(16) Liang, C.; Newton, M. D. *J. Phys. Chem.* **1993**, *97*, 3199−3211.

(17) Beratan, D. N.; Betts, J. N.; Onuchic, J. N. *Science* **1991**, 252, 1285−1288.

(18) Miller, N. E.; Wander, M. C.; Cave, R. J. *J. Phys. Chem. A* **1999**, *103*, 1084−1093.

(19) Gu, Y.; Kumar, K.; Lin, Z.; Read, I.; Zimmt, M. B.; Waldeck, D. H. *J. Photochem. Photobiol., A* **1997**, *105*, 189−196.

(20) Kumar, K.; Kurnikov, I. V.; Beratan, D. N.; Waldeck, D. H.; Zimmt, M. B. *J. Phys. Chem. A* **1998**, *102*, 5529−5541.

(21) Lokan, N. R.; Craig, D. C.; Paddon-Row, M. N. *Synlett* **1999**, 397−400.

(22) Read, I.; Napper, A.; Kaplan, R.; Zimmt, M. B.; Waldeck, D. H. *J. Am. Chem. Soc.* **1999**, *121*, 10976−10986.

(23) Sakata, Y.; Tsue, H.; O'Neil, M. P.; Wiederrecht, G. P.; Wasielewski, M. R. *J. Am. Chem. Soc.* **1994**, *116*, 6904−6909.

(24) Newton, M. D. *J. Electroanal. Chem.* **1997**, *438*, 3−10.

(25) Hayashi, S.; Kato, S. *J. Phys. Chem. A* **1998**, *102*, 3333−3342.

(26) Weidemaier, K.; Tavernier, H. L.; Swallen, S. F.; Fayer, M. D. *J. Phys. Chem. A* **1997**, *101*, 1887−1902.

(27) Miller, J. R. *J. Phys. Chem.* **1975**, *79*, 1070−1078.

(28) Guarr, T.; McGuire, M. E.; McLendon, G. *J. Am. Chem. Soc.* **1985**, *107*, 5104−5111.

10.1021/ja000017h CCC: $19.00

kinetics data. In a typical experiment, a small concentration of electron or hole donors is embedded in a glassed solvent amid a higher concentration of randomly distributed acceptors. The donor is a photoexcited chromophore or a radiolytically generated radical. The time-dependent survival probability of the donor depends on the concentration of the acceptors, the rate constant for electron/hole transfer when D and A are in van der Waals contact (k_0), and the distance decay factor β. Extracting reliable values for k_0 and β from time-resolved spectroscopic measurements, however, can be rather difficult because the two parameters are highly correlated.[26,29] For the case of photoinitiated ET in glasses, measurements of luminescence decay kinetics and luminescence quantum yields at several different quencher concentrations provide enough information to decouple k_0 and β, permitting reliable values to be determined for each parameter.[26]

Of the many solvents that could be examined, water enjoys a unique position as a medium for electron transfer. Aqueous-solution redox processes pervade chemistry and biology, and ET reactions in water have been among the most intensively studied.[30−32] The high dielectric constant of water has long been recognized to impose large reorganization barriers to ET,[31] but little is known about its ability to mediate long-range couplings.[20,24,25] In 1984, Larsson suggested that long-range ET in water would be inefficient ($\beta = 2.4$ $Å^{-1}$) because of the large energy gap between the hole states of water and those of D and A.[33] More recent theoretical treatments, however, have produced β values in the 1.0−1.8 $Å^{-1}$ range.[18,24,34] Experimental investigations have not fared much better in defining β. Pulse radiolysis studies of ET in aqueous glasses have been interpreted in terms of β values between 0.5 and 1.4 $Å^{-1}$,[27,35] while a value of 0.75 $Å^{-1}$ was extracted from transient conductance measurements in fluid solution.[36] There is clearly no consensus from theory or experiment about the effectiveness of water as a tunneling medium. We have, therefore, investigated ET in aqueous acidic glasses in order to define β values for these media.

Photoinitiated electron tunneling in rigid solvents at cryogenic temperatures is possible only with carefully chosen donors and acceptors. It is difficult to prevent pure water from crystallizing at low temperatures, but concentrated aqueous acidic solutions (>20% v/v) will vitrify when cooled to 77 K. The first requirement for D and A, then, is thermal and photochemical stability in strong acids. ET reactions that proceed readily in fluid polar solutions often slow dramatically when the solvent is frozen. Excited-state ET reactions in glasses usually cannot compete with radiative and other nonradiative decay processes. This behavior is attributed to the inability of the rigid solvent to stabilize the D^+/A^- charge distribution, effectively reducing the driving force for the reaction.[37] To sustain efficient ET in low-temperature glasses, the fluid solution reaction must be highly exergonic. We have found that the D/A pair $Ru(tpy)_2^{2+}/Fe(OH_2)_6^{3+}$, with a *D to A ET driving force greater than 1.5 eV in fluid aqueous solution, is well suited for study.

Experimental Procedures

Materials. $[Ru(tpy)_2]Cl_2$ (tpy = 2,2′:6,2″-terpyridine) was synthesized and purified according to published procedures.[38] The following were used without further purification: $[Ru(bpy)_3]Cl_2$ (bpy = 2,2′-bipyridine) (>98%), $(NH_4)Fe(SO_4)_2$ (99.99%), H_2SO_4 (doubly distilled), D_2O (99.9%), D_2SO_4 (99.9%) (Aldrich); $[Ru(NH_3)_6]Cl_3$ (>99%) (Strem); and HSO_3F (>97%) (Fluka).

Glassing Solvents. Stock solutions of 25% v/v acid (H_2SO_4, HSO_3F in H_2O, and D_2SO_4 in D_2O) containing ∼10 μM $[Ru(tpy)_2]Cl_2$ were prepared for each experiment. A 0.5 M $(NH_4)Fe(SO_4)_2$ solution was prepared with the $[Ru(tpy)_2]Cl_2$ stock solution, and serial dilution (also with the $[Ru(tpy)_2]Cl_2$ stock solution) gave $Fe(H_2O)_6^{3+}$ concentrations in the 0−0.5 M range. This procedure ensured identical concentrations of $Ru(tpy)_2^{2+}$ for all the samples in a series. The solutions were degassed with Ar for 5 min in a 5 mm o.d. tube that fit into a liquid nitrogen finger dewar (Wilmad). The samples were frozen slowly (dipping rate ∼ 0.2 cm/s) in liquid nitrogen to minimize crack formation in the aqueous glasses.

Methods

Quantum Yields. The 514.5 nm wavelength line from an argon ion laser (Coherent Innova 70) was used to excite $Ru(tpy)_2^{2+}$ embedded in the glasses. The luminescence was dispersed by a 0.75 m spectrograph (Spex 750M) and detected with a liquid-nitrogen-cooled CCD (Princeton Instruments). The CCD provided accurate luminescence intensity measurements over three orders of magnitude; a large range of quencher concentrations (0−0.5 M) could be spanned without changing instrument parameters. Quantum-yield measurements in glasses are very sensitive to sample positioning and the homogeneity of the glasses. Small fractures in the glasses gave rise to large deviations in the measured luminescence intensities. To minimize these intensity fluctuations, the finger dewar containing the sample was placed in a homemade integrating sphere constructed from a 1 L frosted round-bottom flask. A steady flow of nitrogen gas eliminated condensation on the optical faces. Quantum-yield measurements were repeated at least three times; with care, intensity fluctuations could be kept to the ∼1% (SD/mean) level. To test our ability to reproducibly position samples, both steady-state and time-resolved fluid solution Stern−Volmer quenching experiments were performed with $Ru(bpy)_3^{2+}$ as the chromophore and $Ru(NH_3)_6^{3+}$ as the quencher. We obtained excellent linear correlations ($R = 0.9999$) when the integrated luminescence intensity was plotted against luminescence lifetime.

Luminescence Decay Kinetics. Samples were excited at 10 Hz with 10 ps, 532 nm pulses from a regeneratively amplified mode-locked Nd:YAG laser.[39] The luminescence was dispersed through a monochromator (Spex 270M) onto a photomultiplier tube (PMT) (Hamamatsu R928). The PMT current was amplified and recorded with a transient digitizer (LeCroy 9354A).

Data Analysis. The luminescence decay kinetics ($I(t)$) for a chromophore embedded in a rigid face-centered-cubic lattice with nearest neighbor distance d, surrounded by a random distribution of ET quenchers at lattice points is given by eq 1.[40,41]

$$\ln\left(\frac{I(t)}{I(t{=}0)}\right) = \ln(I_0(t)) - \sum_{j=1}^{\infty}\left(\frac{[Q]d^3}{2348}\right)^j {}^1\!/_j \sum_i{}' [1 - \exp(-k_0 t \exp[-\beta(R_i - b)])] \quad (1)$$

---

(29) Swallen, S. W.; Weidemaier, K.; Tavernier, H. L.; Fayer, M. D. *J. Phys. Chem.* **1996**, *100*, 8106−8117.

(30) Bertini, I.; Gray, H. B.; Lippard, S. J.; Valentine, J. S. *Bioinorganic Chemistry*; University Science Books: Mill Valley, CA, 1994.

(31) Marcus, R. A.; Sutin, N. *Biochim. Biophys. Acta* **1985**, *811*, 265−322.

(32) Bard, A. J.; Faulkner, L. R. *Electrochemical Methods*; John Wiley & Sons: New York, 1980.

(33) Larsson, S. *J. Phys. Chem.* **1984**, *88*, 1321−1323.

(34) Benjamin, I.; Evans, D.; Nitzan, A. *J. Chem. Phys.* **1997**, *106*, 6647−6654.

(35) Alexandrov, I. V.; Khairutdinov, R. F.; Zamarev, K. I. *Chem. Phys.* **1978**, *32*, 123−141.

(36) Schmidt, K. H.; Han, P.; Bartels, D. M. *J. Phys. Chem.* **1995**, *99*, 10530−10539.

(37) Wasielewski, M. R.; Johnson, D. G.; Svec, W. A.; Kersey, K. M.; Minsek, D. W. *J. Am. Chem. Soc.* **1988**, *110*, 7219−7221.

(38) Lin, C.-T.; Böttcher, W.; Chou, M.; Creutz, C.; Sutin, N. *J. Am. Chem. Soc.* **1976**, *98*, 6536−6544.

(39) Bachrach, M. Ph.D. Thesis, California Institute of Technology, 1996.

(40) Blumen, A.; Manz, J. *J. Chem. Phys.* **1979**, *71*, 4694−4702.

(41) Blumen, A. *J. Chem. Phys.* **1980**, *72*, 2632−2640.

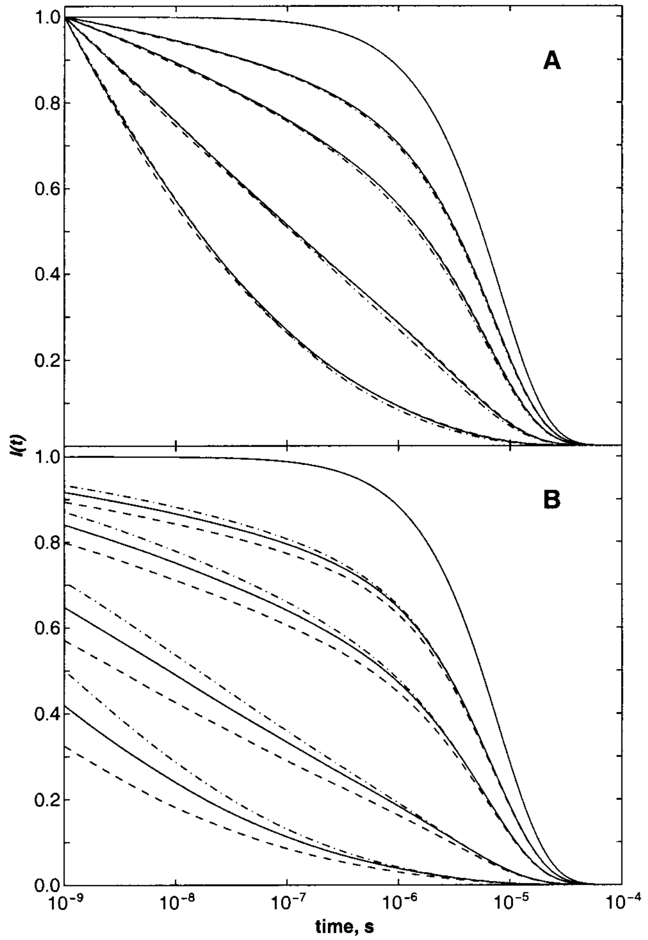

Figure 1. Simulated luminescence decay kinetics calculated using eq 1 ($b = 4$; $d = 2$; $I_0(t) = \exp(-t/\tau_0)$; $\tau_0 = 8 \times 10^{-6}$ s) with three different pairs of k_0 and β values (2×10^{11} s^{-1}, 1.35 Å^{-1} (- – -); 10^{12}, 1.50 (—); 7.5×10^{12}, 1.65 (- - -)); [Q] = 0.0, 0.05, 0.1, 0.25, 0.50 M (upper to lower); (A) luminescence intensities are normalized to the earliest calculated time point (10^{-9} s); (B) intensities are scaled according to luminescence quantum yields.

The luminescence decay, relative to its value at time zero ($I(t{=}0)$), depends on the luminescence decay kinetics in the absence of quencher ($I_0(t)$), the distance decay factor (β), and the ET rate (k_0) at contact distance (b) between luminophore ($Ru(tpy)_2^{2+}$) and quencher ($Fe(OH_2)_6^{3+}$) molecules. The sum over lattice points i excludes the origin (luminophore) and any lattice points closer than b. The factor of 2348 is appropriate for quencher concentrations ([Q]) measured in moles per liter and distances in angstroms. The sum over j can be truncated after the first term for [Q] < 5 M.[41]

The goal of this analysis is to determine the ET distance decay factor, β, from luminescence decay kinetics measured at several different quencher concentrations. As written, eq 1 contains three unknown parameters: β, k_0, and $I(t{=}0)$. Variations in laser power and sample positioning lead to different values of $I(t{=}0)$ for each quencher concentration. Since a significant amount of quenching occurs on the subnanosecond time scale, the 5 ns time resolution of our instrument prevents direct measurement of $I(t{=}0)$. When luminescence kinetics data are normalized to the intensity of the earliest measured time point, the two remaining parameters, β and k_0, are strongly correlated and a unique solution cannot be found (Figure 1a).[29] Independent measurements of $I(t{=}0)$ are necessary to decouple β and k_0.[26] Measurements of luminescence quantum yields, relative to an unquenched sample, provided time-integrated luminescence intensities, permitting accurate scaling of the time-resolved data. With properly scaled luminescence kinetics data, it is possible to extract reliable values for β and k_0 (Figure 1b). Quantum-yield-normalized decay kinetics for quencher-containing samples were used in all fitting procedures. There were some variations in best-fit β and k_0 values for different quencher concentrations. These fluctuations were likely the result of errors in scaling the time-resolved luminescence data.

Table 1. Best-Fit Values of β and k_0 (Eq 2)[a] Extracted from Luminescence Decay Kinetics and Quantum Yields of $Ru(tpy)_2^{2+}$ Quenched by $Fe(OH_2)_6^{3+}$ in Aqueous Acidic Glasses at 77 K

solvent[b]	$[Fe(OH_2)_6^{3+}]$, M	β, Å^{-1}	k_0, s^{-1}
H_2SO_4	0.05	1.74	5.7×10^{13}
	0.10	1.65	1.6×10^{13}
	0.25	1.63	1.1×10^{13}
	0.50	1.71	3.9×10^{13}
$HFSO_3$	0.05	1.78	9.4×10^{13}
	0.10	1.72	4.7×10^{13}
	0.25	1.60	6.1×10^{12}
	0.50	1.61	5.3×10^{12}
D_2SO_4	0.05	1.64	8.4×10^{12}
	0.10	1.61	6.7×10^{12}
	0.25	1.67	1.6×10^{13}
	0.50	1.57	1.4×10^{12}

[a] Scaled kinetics fit to eq 2 with $b = 4$ Å. [b] Acidic glasses were 25% v/v.

Data were fit to eq 1 using a Levenberg–Marquardt algorithm[42] with two adjustable parameters (β, k_0) to minimize the sum of squared relative deviations between calculated and observed luminescence intensities ($\chi_{\mathrm{rel}}^2 = \sum[I_{\mathrm{calc}} - I_{\mathrm{obsd}}]^2/[(N-2)I_{\mathrm{obsd}}^2]$, where N = number of data points). Better fits resulted when an experimental decay function was used for $I_0(t)$ rather than an exponential function. The quality of the fits also depended on the magnitudes of b and d; χ_{rel}^2 became smaller as the two parameters decreased. For values of $b \leq 5$ Å and $d \leq 3$ Å, χ_{rel}^2 reached minimum values; for $b \leq 4$ Å, β and k_0 approached limiting values.

Given the dependence of χ_{rel}^2 on d, we also examined the continuum limit for the acceptor distribution. The low-concentration limiting form of the discrete-lattice model described by eq 1 can be generalized to a continuous medium, replacing sums with integrals, yielding eq 2.[41]

$$\ln\left(\frac{I(t)}{I(t{=}0)}\right) = \ln(I_0(t)) - \left(\frac{[\mathrm{Q}]}{132.12}\right)\int_b^{\infty}[1 - \exp(-k_0 t \exp[-\beta(R - b)])]R^2\,\mathrm{d}R \quad (2)$$

This equation is analogous to expressions developed earlier[43,44] but accounts for the finite volume of the chromophore. The factor of 132.12 is appropriate for quencher concentrations measured in moles per liter and distances measured in angstroms. Data were fit using the same minimization algorithm and criteria employed for eq 1. Overall, the continuous model (eq 2) gave slightly better fits than the discrete-lattice model (eq 1) for $d \geq 3$. Fits to eq 2 gave results that were virtually identical with those obtained with eq 1, using $d = 2$. The best-fit values of β (1.60–1.75 Å^{-1}) again approached lower limits for $b \leq 4$ Å. It is clear from eqs 1 and 2 that the magnitude of k_0 is coupled to the value of b. The results reported in Table 1 correspond to fits to eq 2 using $b = 4$. Detailed fitting results using eq 2 for $^*Ru(tpy)_2^{2+}$ quenched by $Fe(OH_2)_6^{3+}$ in 25% H_2SO_4, D_2SO_4, and $HFSO_3$ are given in the Supporting Information.

Results and Discussion

In the absence of quenchers, the luminescence lifetime of $Ru(tpy)_2^{2+}$ is 8.0 μs in H_2SO_4/H_2O and HSO_3F/H_2O glasses (25% v/v) at 77 K and 10.2 μs in D_2SO_4/D_2O (25% v/v). In contrast to $Ru(bpy)_3^{2+}$, $Ru(tpy)_2^{2+}$ does not display any thermal or photochemical reactivity in these strongly acidic media. We examined several organic electron acceptors (methylviologen,

---

(42) Press, W. H.; Vetterling, W. T. *Numerical Recipes in FORTRAN: The Art of Scientific Computing*, 2nd ed.; Cambridge University Press: New York, 1992.

(43) Inokuti, M.; Hirayama, F. *J. Chem. Phys.* **1965**, *43*, 1978–1989.

(44) Thomas, D. G.; Hopfield, J. J.; Augustyniak, W. M. *Phys. Rev.* **1965**, *140*, A202–A220.

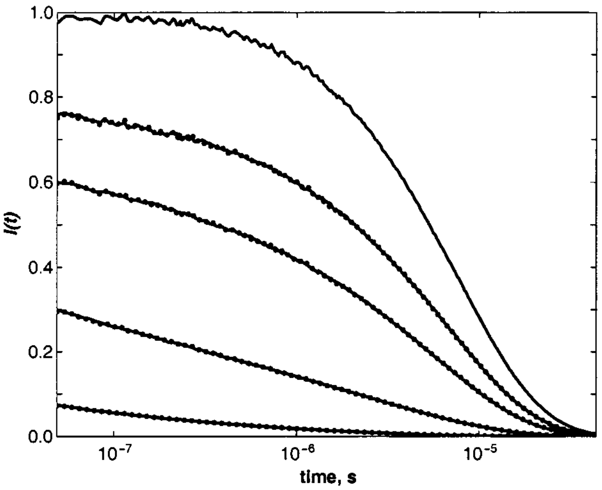

Figure 2. Luminescence decay kinetics for $Ru(tpy)_2^{2+}$ in a H_2SO_4/H_2O glass (at 77 K) in the presence of $Fe(OH_2)_6^{3+}$ (upper to lower traces: 0.0, 0.05, 0.10, 0.25, 0.50 M). Dots correspond to calculated decays using eq 1 and the parameters listed in Table 1.

tetracyanoethylene, benzoquinone) and found that they do not quench $^*Ru(tpy)_2^{2+}$ luminescence in the frozen glasses. The addition of moderate concentrations of the powerfully oxidizing $Fe(OH_2)_6^{3+}$ ion (0.01−0.5 M, $E° = 0.77$ V versus NHE[38]) to the glasses, however, leads to accelerated and highly nonexponential $^*Ru(tpy)_2^{2+}$ decay kinetics. Electron transfer is the most likely mechanism for this quenching. In fluid solution, for example, $Fe(OH_2)_6^{3+}$ quenches excited $Ru(bpy)_3^{2+}$ by electron transfer with a rate constant close to the diffusion limit (2.7×10^9 M^{-1} s^{-1}).[38] Dipole−dipole energy-transfer quenching[45] will be very inefficient because the spectral overlap of the $Fe(OH_2)_6^{3+}$ absorption ($\lambda_{max} = 794$ nm, $\epsilon = 0.1$ M^{-1} cm^{-1}; $\lambda_{max} = 540$ nm, $\epsilon = 0.1$ M^{-1} cm^{-1} [46]) and the $Ru(tpy)_2^{2+}$ luminescence ($\lambda_{max} = 600$ nm) is negligible. Electron exchange energy transfer is unlikely to be competitive because the distance decay factor for this process should be twice that for ET.[47]

Distance decay constants for $Fe(OH_2)_6^{3+}$ quenching of $^*Ru(tpy)_2^{2+}$ in aqueous glasses were extracted from measurements of luminescence decay kinetics (Figure 2) as functions of quencher concentration. The luminescence lifetime of $^*Ru(tpy)_2^{2+}$ in aqueous glasses is long enough to allow a significant distance range (∼25 Å) to be probed. Because quantum-yield data were used to scale the intensities of the decay kinetics, only two parameters (Table 1) were required to fit the data. We find that a distance decay constant of 1.68 ± 0.07 $Å^{-1}$ adequately describes ET in the three different glasses and that the rate constants for ET at van der Waals contact are near 10^{13} s^{-1}. The 1.7 eV driving force for $^*Ru(tpy)_2^{2+}$/$Fe(OH_2)_6^{3+}$ ET in fluid solution is evidently great enough to compensate for the loss of product stabilization in the glass matrix. Although large concentrations of acid (25% v/v) are required for vitrification, water is still the dominant component in these matrices. On a molar basis, the acidic glasses are >90% H_2O/H_3O^+. The fact that the distance decay parameter in the HSO_3F glass is virtually identical with that obtained in the H_2SO_4 glass provides additional evidence that the oxo anions are not playing an important coupling role.[48]

Our results provide an interesting comparison to some early ET studies in organic glasses. Pulse radiolysis initiated ET from the biphenyl radical anion to a variety of organic acceptors in 2-methyltetrahydrofuran (MTHF) glasses at 77 K has been interpreted in terms of $\beta = 1.20$ $Å^{-1}$.[4] In these studies, the donor survival probability was probed directly by transient absorption spectroscopy; consequently, the β and k_0 values extracted from the kinetics data were not strongly correlated. Superexchange coupling models suggest that two factors are important in bridge-mediated ET: the coupling between adjacent units in the bridge; and the energy gap between the tunneling electron and the hole/electron states of the bridge.[13] The individual bridge elements in water are coupled via hydrogen-bonded interfaces. Several experimental investigations have shown that hydrogen-bond-mediated ET is quite efficient.[49−56] The extensive network of hydrogen bonds in liquid water, therefore, should provide stronger coupling between adjacent bridge elements than that found in MTHF.

The significantly greater β value for ET in water compared to MTHF is likely the manifestation of a larger tunneling-energy gap. The far UV absorption spectra of water and THF provide indirect measures of these energy gaps. The onset of UV absorption in THF is 6.2 eV (200 nm), with the first maximum appearing at 6.6 eV (188 nm).[57] The band gap in water is significantly larger; absorption begins at 7 eV (177 nm), and the first maximum is at 8.2 eV (151 nm).[58] It is difficult to locate the energy of the tunneling electron at the transition state nuclear configuration in relation to these solvent band gaps, particularly for reactions in rigid media. Nevertheless, the solvent band gaps should provide a first approximation to the tunneling-energy gap for long-range ET, and the larger β value for ET in water is consistent with its larger band gap.

The β values that we have found for ET in aqueous glasses (Table 1) are in excellent agreement with calculations that suggest the ET distance-decay constant in water is in the 1.5−1.8 $Å^{-1}$ range.[18] These calculations support Larsson's initial suggestion that tunneling through water would be unfavorable, owing to the large tunneling-energy gap.[33] The β values previously reported for ET in aqueous glasses are comparable to or lower than those of saturated organic bridges (0.5−1.4 $Å^{-1}$), which would suggest an important role for coupling through the solvent in long-range ET. Our results, however, show clearly that water is a poor medium for electron transfer. In addition to the large reorganization barriers associated with ET in water, we must add the penalty associated with poor electronic coupling.

---

(45) Förster, T. *Ann. Phys. (Leipzig)* **1948**, *2*, 55−75.

(46) Jørgensen, C. K. *Acta Chem. Scand.* **1954**, *8*, 1502−1512.

(47) Closs, G. L.; Piotrowiak, P.; Macinnis, J. M.; Fleming, G. R. *J. Am. Chem. Soc.* **1988**, *110*, 2652−2653.

(48) Additionally, there is no hydrogen/electron donor (H/D) isotope effect on coupling (i.e., solvent deuteration has a negligible effect on the measured distance decay factors ($\beta_H/\beta_D = 1.003 \pm 0.02$)).

(49) Wuttke, D. S.; Bjerrum, M. J.; Winkler, J. R.; Gray, H. B. *Science* **1992**, 256, 1007−1009.

(50) Regan, J. J.; Di Bilio, A. J.; Langen, R.; Skov, L. K.; Winkler, J. R.; Gray, H. B.; Onuchic, J. N. *Chem. Biol.* **1995**, *2*, 489−496.

(51) de Rege, P. J. F.; Williams, S. A.; Therien, M. J. *Science* **1995**, 269, 1409−1413.

(52) Kirby, J. P.; Roberts, J. A.; Nocera, D. G. *J. Am. Chem. Soc.* **1997**, *119*, 9230−9236.

(53) Yang, J.; Seneviratne, D.; Arbatin, G.; Andersson, A. M.; Curtis, J. C. *J. Am. Chem. Soc.* **1997**, *119*, 5329−5336.

(54) Asano-Someda, M.; Levanon, H.; Sessler, J. L.; Wang, R. Z. *Mol. Phys.* **1998**, *95*, 935−942.

(55) Regan, J. J.; Ramirez, B. E.; Winkler, J. R.; Gray, H. B.; Malmström, B. G. *J. Bioenerg. Biomembr.* **1998**, *30*, 35−39.

(56) Babini, E.; Bertini, I.; Borsari, M.; Capozzi, F.; Luchinat, C.; Zhang, X.; Moura, G. L. C.; Kurnikov, I. V.; Beratan, D. N.; Ponce, A.; Di Bilio, A. J.; Winkler, J. R.; Gray, H. B. *J. Am. Chem. Soc.* **2000**, *122*, 4532−4533.

(57) Bremmer, L. J.; Curtis, M. G.; Walker, I. C. *J. Chem. Soc., Faraday Trans.* **1991**, *87*, 1049−1055.

(58) Bernas, A.; Ferradini, C.; Jay-Gerin, J.-P. *Chem. Phys.* **1997**, *222*, 151−160.

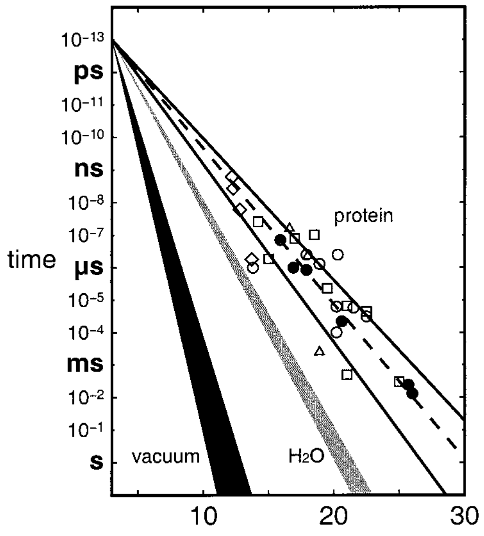

Figure 3. Tunneling timetable for ET in Ru-modified proteins: azurin (●);[8] cytochrome *c* (○);[10] myoglobin (△);[10] cytochrome b_{562} (□);[59] HiPIP (◇).[56] Solid lines illustrate tunneling pathway predictions for coupling along β-strands ($\beta = 1.0$ Å^{-1}) and α-helices ($\beta = 1.3$ Å^{-1}); dashed line illustrates a 1.1 Å^{-1} distance decay.[10] Distance decay for electron tunneling through water is shown as a gray wedge ($\beta = 1.61-1.75$ Å^{-1}). Estimated distance dependence for tunneling through vacuum is shown as the black wedge ($\beta = 3.0-4.0$ Å^{-1}).

The results from a variety of long-range ET measurements are summarized in Figure 3. ET rates in D−br−A complexes with saturated alkane spacers are best described by an exponential distance decay constant of 0.9 Å^{-1}.[9] The 1.2 Å^{-1} decay found in MTHF can be explained by weaker coupling between bridge elements in the solvent than in the covalently bonded alkane chain. An exponential distance decay constant of 1.1 Å^{-1} provides a reasonable first approximation to a broad set of data from Ru-modified proteins.[8,10,59] The scatter of the measured rates around the exponential decay line can be attributed to the fact that a protein does not provide a homogeneous tunneling barrier; the secondary and tertiary structure of the protein must be taken into account in order to understand long-range couplings.[60] The region representing the distance decay for coupling through water ($\beta = 1.61-1.75$ Å^{-1}) demonstrates that, although better than that through a vacuum ($\beta = 3-4$ Å^{-1}), tunneling 20 Å through water is at least 100 times slower than tunneling through protein or hydrocarbon bridges. Exclusion of water from the space between redox centers is a key factor in maximizing the efficiency of long-range ET in biological molecules and assemblies.

Acknowledgment. We thank D. N. Beratan, R. J. Cave, N. S. Lewis, R. A. Marcus, J. R. Miller, and M. D. Newton for helpful discussions. This research was supported by NSF Grant CHE9610164 and the Arnold and Mabel Beckman Foundation.

Supporting Information Available: Plots of fitting results using eq 2 for *Ru(tpy)$_2^{2+}$ quenched by Fe(OH$_2$)$_6^{3+}$ in 25% H_2SO_4, D_2SO_4, and $HFSO_3$ as functions of *b*; luminescence decay kinetics and fits to eq 1 for Ru(tpy)$_2^{2+}$ in $HFSO_3/H_2O$ and D_2SO_4/D_2O glasses (77 K) in the presence of Fe(OH$_2$)$_6^{3+}$ (PDF). This information is available free of charge via the Internet at http://pubs.acs.org.

JA000017H

---

(59) Winkler, J. R.; Di Bilio, A.; Farrow, N. A.; Richards, J. H.; Gray, H. B. *Pure Appl. Chem.* **1999**, *71*, 1753−1764.

(60) Winkler, J. R. *Curr. Opin. Chem. Biol.* **2000**, *4*, 192−198.